JSHC
Japan Society of
Histochemistry and Cytochemistry
Established 1959

Acta Histochem. Cytochem. 48 (2): 37–45, 2015
doi: 10.1267/ahc.14046

Localization of Core Planar Cell Polarity Proteins, PRICKLEs, in Ameloblasts of Rat Incisors: Possible Regulation of Enamel Rod Decussation

Sumio Nishikawa[1] and Tadafumi Kawamoto[2]

[1]Department of Biology, Tsurumi University School of Dental Medicine, Yokohama, Japan and [2]Radioisotope Research Institute, Tsurumi University School of Dental Medicine, Yokohama, Japan

Received September 16, 2014; accepted March 6, 2015; published online April 16, 2015

To confirm the possible involvement of planar cell polarity proteins in odontogenesis, one group of core proteins, PRICKLE1, PRICKLE2, PRICKLE3, and PRICKLE4, was examined in enamel epithelial cells and ameloblasts by immunofluorescence microscopy. PRICKLE1 and PRICKLE2 showed similar localization in the proliferation and secretory zones of the incisor. Immunoreactive dots and short rods in ameloblasts and stratum intermedium cells were evident in the proliferation to differentiation zone, but in the secretion zone, cytoplasmic dots decreased and the distal terminal web was positive for PRICKLE1 and PRICKLE2. PRICKLE3 and PRICKLE4 showed cytoplasmic labeling in ameloblasts and other enamel epithelial cells. Double labeling of PRICKLE2 with VANGL1, which is another planar cell polarity protein, showed partial co-localization. To examine the transport route of PRICKLE proteins, PRICKLE1 localization was examined after injection of a microtubule-disrupting reagent, colchicine, and was compared with CX43, which is a membrane protein transported as vesicles via microtubules. The results confirmed the retention of immunoreactive dots for PRICKLE1 in the cytoplasm of secretory ameloblasts of colchicine-injected animals, but fewer dots were observed in control animals. These results suggest that PRICKLE1 and PRICKLE2 are transported as vesicles to the junctional area, and are involved in pattern formation of distal junctional complexes and terminal webs of ameloblasts, further implying a role in the formed enamel rod arrangement.

Key words: ameloblast, PRICKLE, planar cell polarity, immunohistochemistry, rat incisor

I. Introduction

Ameloblasts are responsible for tooth enamel formation. In the rat incisor, amelogenesis progresses continuously throughout the animal's life, beginning from the proliferation zone of enamel epithelial cells at the labial and apical ends of the tooth [35]. After progression of amelogenesis, inner enamel epithelial cells differentiate and then secrete enamel proteins as secretory ameloblasts. These secretory ameloblasts are classified into inner and outer enamel-secretory phases. Inner enamel secretory ameloblasts form rows, with each row moving to the left and right, alternatively, in addition to backwards and incisally, resulting in enamel rod decussation. Outer enamel secretory ameloblasts move backwards and incisally, but cease to move sideways, resulting in the straight-coursed enamel rod alignment. After the secretory phase, ameloblasts enter the maturation phase, shortening their height, and performing resorption of enamel matrices and elevation of mineralization. Secretory ameloblasts have junctional complexes such as desmosomes, tight junctions, gap junctions, and adherens junctions at the proximal and distal cell ends [1, 16, 17, 24, 25]. Cross sectioned cell profiles at the level of proximal junctional complexes exhibit circular actomyosin bundles in secretory ameloblasts referred to as proximal terminal web (PTW). In contrast, actomyosin filament bundles at the level of distal junctional complexes, referred to as distal terminal web (DTW), differ in shape

Correspondence to: Sumio Nishikawa, Department of Biology, Tsurumi University School of Dental Medicine, 2–1–3 Tsurumi, Tsurumi-ku, Yokohama 230–8501, Japan. E-mail: nishikawa-s@tsurumi-u.ac.jp

between inner and outer enamel-secretory ameloblasts. Tetragonal distribution of actomyosin bundles is observed in the former and pentagonal or hexagonal distribution of bundles is observed in the latter [15, 16, 36]. At the level of distal junctions of the inner enamel secretory ameloblasts, there is anisotropic distribution of actomyosin bundles. Actomyosin bundles are abundant in the orthogonal plane of the long incisor axis, referred to as major web [9], but are sparse in the plane along the long incisor axis, referred to as minor web. In the outer enamel secretory ameloblasts, the distribution of actomyosin bundles is isotropic around the distal junction. These different shapes at the level of distal junctional complexes are thought to be related to differences in formed enamel rod arrangement [15, 16, 36].

Planar cell polarization, which appears in the plane perpendicular to the apicobasal axis of epithelial cells [26, 31, 33], may be responsible for the differences in shape of ameloblasts. It is reasonable to suggest that core PCP proteins play a role in actin-based filament bundle formation at the distal terminal web and enamel rod decussation [21]. Core planar cell polarity (PCP) proteins are Frizzled (FZD), Vang-like protein (VANGL), Dishevelled (DVL), PRICKLE, ankyrin repeat domain 6 (ANKRD6), and cadherin EGF LAG seven-pass G-type receptor (CELSR). These genes and proteins are widely expressed from Drosophila to vertebrates [31]. These planar cell polarity proteins are mediators of one of the non-canonical Wnt pathways: the Wnt/planar-cell-polarity pathway. Wnt5a is a typical non-canonical Wnt family member, and its receptors FZD4, FZD6, LRAP5, and Ror2 are reportedly localized in dental epithelia [14, 23, 34]. Wnt5a-deficient animals show retardation of tooth development [14].

PRICKLE proteins are known to interact with VANGL membrane proteins. VANGL recruits PRICKLE proteins, and conversely, PRICKLE proteins promote aggregation of VANGL-PRICKLE complexes at the plasma membrane [7, 26]. Importantly, PRICKLE proteins inhibit another set of core planar cell polarity proteins: DVL and FZD. FZD is a membrane protein that recruits DVL. PRICKLE causes reductions in membrane localization of DVL. Thus, PRICKLE inhibits FZD-DVL signaling. Interestingly, another DVL-binding protein, Diego, competes with PRICKLE, exerting an inhibitory effect against VANGL-PRICKLE signaling [26]. FZD, VANGL, and CELR are known to be localized in the rat incisor [21]. However, localization of DVL and PRICKLE is unclear at present, although transcripts of PRICKLE are known to be present in the teeth [11]. Some epilepsy patients with heterozygous mutations of PRICKLEs [30] and PRICKLE3 localization in centrioles [6] have been reported. Determination of PRICKLE protein localization is the aim of the present study.

In this study, we examined the localization of PRICKLE1, PRICKLE2, PRICKLE3, and PRICKLE4. Because of similarities between the localization of PRICKLE1 and PRICKLE2 and that of gap junction protein CX43, similar transportation pathways for PRICKLE and CX43 proteins were suspected. CX43 has been shown to be transported via microtubules to the plasma membrane [27]. Thus, CX43 localization was examined and compared with PRICKLE1 localization with and without injection of colchicine, which is a microtubule-disruptive reagent.

II. Materials and Methods

Nine-day-old Jcl Wistar rats (CLEA Japan, Tokyo, Japan) were sacrificed under deep anesthesia and rapidly frozen, and freeze-dried sections (5 μm thick) were obtained without fixation or demineralization according to the method of Kawamoto [10]. The Principles of Laboratory Animal Care (NIH publication No. 85-23, revised 1985) were followed, as well as specific national laws where applicable. All animal experiments were approved by the Institutional Ethics Review Board for animal experiments and its guidelines for animal care were also followed. Sections were labeled with rabbit polyclonal anti-PRICKLE1 antibody (1 μg/ml), anti-PRICKLE2 antibody (2.5 μg/ml), anti-PRICKLE3 (5 μg/ml), anti-PRICKLE4 (6 μg/ml), or anti-connexin 43 (CX43) (10 μg/ml) antibody in 1% bovine serum albumin (BSA) in phosphate buffered saline (PBS), pH 7.3, at 4°C overnight. These antibodies were obtained from Sigma-Aldrich (St. Louis, MO). They were further labeled with Alexa Fluor 488-conjugated anti-rabbit IgG (Invitrogen, Camarillo, CA), Alexa Fluor 647 phalloidin (Invitrogen) diluted 1:50, and 1 μg/ml Hoechst 33342 (Invitrogen) at room temperature for 30 min. Some sections were double labeled with rabbit anti-PRICKLE2 antibody (2.5 μg/ml) and goat anti-VANGL1 antibody (40 μg/mL; G-17, sc-46557; Santa Cruz Biotechnology, Santa Cruz, CA) at 4°C overnight, followed by Alexa Fluor 555-conjugated donkey anti-rabbit IgG (Invitrogen) diluted 1:100, donkey anti-goat IgG-FITC (Santa Cruz) diluted 1:20, Alexa Fluor 647 phalloidin diluted 1:50, and 1 μg/ml Hoechst 33342 at room temperature for 30 min. Negative controls were incubated with 1% BSA-PBS alone instead of anti-VANGL1 and normal rabbit IgG in 1% BSA-PBS instead of anti-PRICKLEs and CX43 antibodies.

Twelve male Jcl Wistar rats (age, 4 weeks; 80–85 g; CLEA Japan) were used for colchicine experiments. Colchicine (1.3 mg/kg dosage; 1 mg/ml solution dissolved in 10% ethanol in PBS) was injected subcutaneously into the back skin. Animals were sacrificed at 15 or 39 hr after colchicine injection. Control animals were injected with the same amount of 10% ethanol in PBS or PBS alone. Dissected maxillae and mandibles were fixed with 4% paraformaldehyde solution at 4°C overnight, and were then demineralized with 5% EDTA, pH 7.2, for 3 weeks. After washing with PBS, tissues were infused with 25% sucrose in PBS. They were rapidly frozen and cryosections were prepared using a cryomicrotome (HM505E; Microm, Walldorf, Germany). Tissues were labeled with anti-PRICKLE1, anti-PRICKLE4 and anti-CX43, as mentioned

above. Negative controls were incubated with normal rabbit IgG in 1% BSA-PBS in place of specific antibodies.

All images were obtained with an Olympus AX80 fluorescence microscope equipped with a Charge Coupled Device camera (Quantix KAF1401E; Photometrics, Tucson, AZ) and MetaMorph software (Universal Imaging, Downingtown, PA), as described previously [20]. To improve image quality, 2D deconvolution processing using MetaMorph software was performed for most micrographs.

III. Results

Figures 1–3 were obtained from cryosections of 9-day-old rats without fixation or demineralization. Figure 4 was obtained from cryosections of 4-week-old rats fixed with paraformaldehyde and demineralized with EDTA. Negative control sections showed no specific labeling in dental tissues from incisors.

Localization of PRICKE1, PRICKLE2, PRICKLE3, and PRICKLE4 in ameloblasts

PRICKLE1 was localized in the cytoplasm as immunofluorescent dots in the proliferation zone of the enamel epithelium (Fig. 1A). Immunofluorescent dots increased in the differentiation zone, where columnar inner enamel epithelial cells possessed nuclei at varying heights (Fig. 1B). Provisional stratum intermedium cells exhibited similar immunofluorescent dots in the cytoplasm. In the inner enamel secretory ameloblasts, cytoplasmic immunofluorescent dots decreased, while structures immunoreactive for PRICKLE1 in PTW and DTW were also labeled with F-actin (Fig. 1C). Fluorescent dots in the stratum intermedium cells remained abundant in the secretory zone. Outer enamel secretory and maturation ameloblasts were rarely labeled with anti-PRICKLE1 antibodies (Fig. 1G–I). The basement membrane of the proliferation and differentiation zones was labeled with anti-PRICKLE1 antibodies (Fig. 1A, B), although the significance of this labeling is unclear.

PRICKLE2 was localized in the proliferation and differentiation zones as immunofluorescent dots or short rods (Fig. 1D, E). Provisional stratum intermedium cells exhibited numerous immunofluorescent dots (Fig. 1E). In the early differentiation zone, some immunofluorescent structures for PRICKLE2 were also labeled with F-actin in PTW. Subsequently, after DTW was formed in the differentiation zone, some immunofluorescent dots were co-localized with F-actin in DTW. In inner and outer enamel-secretory ameloblasts, immunofluorescent dots in cytoplasm decreased markedly, but co-localization with actomyosin bundles in DTW was observed (Figs. 1F and 3D). In the maturation zone, immunofluorescent dots and rods were present in the ameloblasts (Fig. 1J). Some immunoreactive dots were localized in the papillary layer cells of the maturation zone (Fig. 1J). In the odontoblast layer, the center of each odontoblast tended to exhibit a bright immunofluorescent dot (Fig. 3A, B), and these immunofluorescent dots formed a line along the odontoblast layer.

The basement membrane of the outer enamel epithelium of the proliferation zone was immunopositive for PRICKLE3 (Fig. 2A), although the significance of this labelling is unclear. Immunofluorescent staining for PRICKLE3 was observed in the middle inner enamel secretion zone to the maturation zone (Fig. 2B, C). Stratum intermedium cells, stellate reticulum cells, outer enamel epithelial cells, and papillary layer cells were the most prominent immunoreactive cells of the enamel organ (Fig. 2B, C). Their cytoplasm was strongly immunofluorescent. Inner enamel-secretory ameloblasts started to exhibit PRICKLE3-immunopositive fine thread-like fluorescence (Fig. 2B). These fluorescent threads became thick and bright, but their number decreased in more advanced zones of enamel secretion. In maturation ameloblasts, weak diffuse cytoplasmic fluorescence was observed. Some singular cells adjacent to the dentin were labeled with anti-PRICKLE3 (Fig. 2D).

Ameloblasts from the initial secretion to the maturation zone were immunoreactive for PRICKLE4 (Fig. 2E–G). Enamel cells other than ameloblasts showed no positive reactivity. Immunoreactive threads or elongated saccules can be seen in the cytoplasm of secretory ameloblasts. Transition and maturation ameloblasts showed similar immunoreactivity as in the secretion zone, but the reactivity decreased gradually (Fig. 2F, G). The cytoplasm in odontoblasts (Fig. 2E, F) and osteoblasts (Fig. 2F) was immunopositive for PRICKLE4.

Double labeling of differentiating pre-ameloblasts and secretory ameloblasts with PRICKLE2 and VANGL1

As described above, strong immunoreactive dots of PRICKLE1 and PRICKLE2 in stratum intermedium cells and differentiating pre-ameloblasts were similar to those of VANGL1 [21]. Therefore, double labeling experiments with PRICKLE2 and VANGL1 were performed. In differentiating pre-ameloblasts, co-localization of PRICKLE2 and VANGL1 was observed as small immunoreactive dots or short rods (Fig. 3A–C). In secretory ameloblasts, immunoreactivity of VANGL1 was detected in junctional complexes of DTW, while immunoreactivity of VANGL1 decreased in cytoplasm (Fig. 3D–F). Inner enamel secretory ameloblasts of DTW were immunoreactive for VANGL1, PRICKLE2, and Alexa Fluor 647 phalloidin for F-actin, thus confirming their co-localization (Fig. 3D).

Localization of PRICKLE1 and PRICKLE4 after colchicine treatment

PRICKLE1-immunoreactive dots were sparsely localized in the cytoplasm of differentiating inner enamel epithelial cells at 15 and 39 hr after colchicine injection (Fig. 4B). In control animals, similar localization was observed (Fig. 4A). In secretory ameloblasts, however, PRICKLE1-immunopositive dots were distributed in the terminal web and tended to decrease in the cytoplasm in ameloblasts

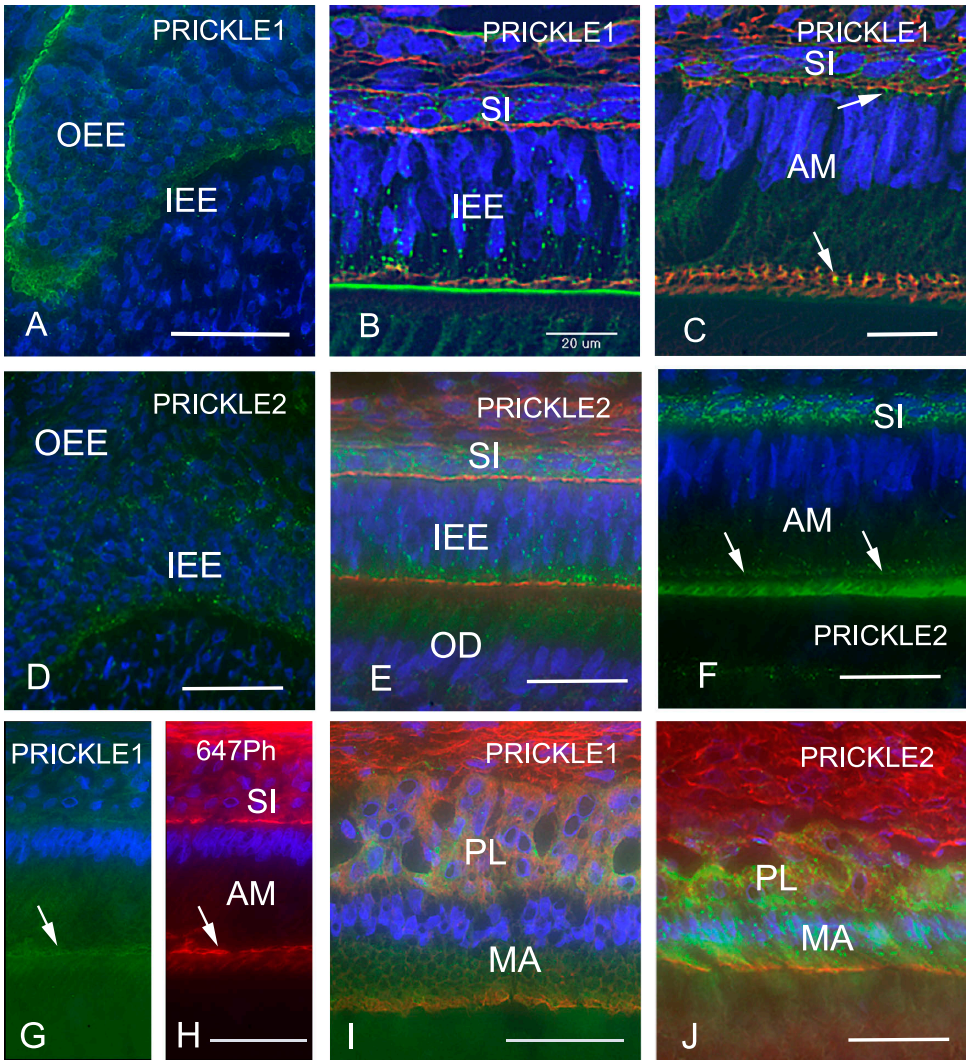

Fig. 1. PRICKLE1 (**A–C, G, I**) and PRICKLE2 (**D–F, J**) localization. Figure (**H**) shows the localization of Alexa Fluor 647 phallodin (647Ph) and Hoechst 33342 (H33342). Nine-day-old rats without fixation or demineralization. Sections were labeled with anti-PRICKLE1 or anti-PRICKLE2 (green), 647Ph (red), and H33342 (blue). (**A, D**) Proliferation zone. Merged image of staining for PRICKLE1 and H33342 (**A**) and for PRICKLE2 and H33342 (**D**). Small PRICKLE1-immunopositive dots (**A**) and PRICKLE2-immunopositive dots (**D**) are present in the cytoplasm of cells. Basement membrane of outer enamel epithelium (OEE) is strongly positive for anti-PRICKLE1 (**A**). (**B, E**) Differentiation zone. Merged image of staining for PRICKLE1, 647Ph, and H33342 (**B**), and for PRICKLE2, 647Ph, and H33342 (**E**). Small PRICKLE1-immunopositive dots (**B**) and PRICKLE2-immunopositive dots (**E**) are present in the inner enamel epithelial cells (IEE) and provisional stratum intermedium cells (SI), and some PRICKLE1-positive dots are co-localized with proximal or distal junction-related F-actin labeled with 647Ph exhibiting yellow color (**B**). (**C, F**) Inner enamel secretory ameloblasts (AM) and stratum intermedium (SI). Merged images of staining for PRICKLE1, 647Ph, and H33342 (**C**), and for PRICKLE2 and H33342 (**F**). Proximal and distal terminal webs (arrows in **C** and **F**) labeled with PRICKLE1 (**C**) and PRICKLE2 (**F**), whereas PRICKLE1-immunopositive dots and PRICKLE2-immunopositive dots in cytoplasm decrease. Upper arrow in (**C**) shows the proximal terminal web. (**G, H**) Outer enamel-secretory ameloblasts labeled with anti-PRICKLE1 and H33342 (**G**) and with 647Ph and H33342 (**H**). Distal terminal web (arrows) is scarcely labeled with anti-PRICKLE1 (**G**). (**I, J**) Maturation ameloblasts (MA) and papillary layer cells (PL). Merged images of staining for PRICKLE1, 647Ph, and H33342 (**I**), and for PRICKLE2, 647Ph, and H33342 (**J**). PRICKLE1 is not positive in ameloblasts and papillary layer cells, whereas many PRICKLE2-immunopositve dots and rods are seen in the cytoplasm of ameloblasts and papillary layer cells. Bars=50 μm (**A, C–J**); 20 μm (**B**).

from control animals (arrowhead, Fig. 4C). On the other hand, numerous PRICKLE1-immunoreactive dots in colchicine-injected rats were distributed in the cytoplasm (arrows, Fig. 4D). Furthermore, secretory ameloblasts showed poor Alexa Fluor 647 phalloidin-positive fluorescence or PRICKLE1-immunoreactive fluorescence in the DTW (arrowhead, Fig. 4D). PRICKLE4 reactivity was observed in the cytoplasm of ameloblasts from colchicine-treated animals, and was similarly observed in the ameloblasts from control animals (not shown).

Gap junction protein CX43 localization after colchicine treatment

Gap junction protein CX43 is known to be localized in differentiating pre-ameloblasts and secretory ameloblasts in a similar pattern as PRICKLE1 and PRICKLE2 [3, 5, 8,

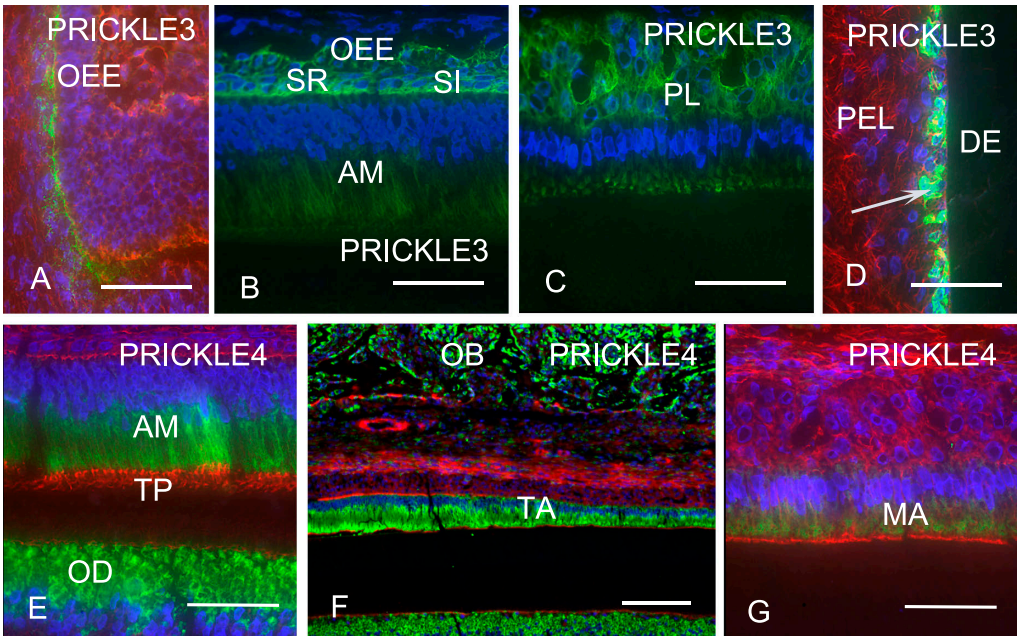

Fig. 2. PRICKLE3 (**A–D**) and PRICKLE4 (**E–G**) localization. Nine-day-old rats without fixation or demineralization. Sections were labeled with anti-PRICKLE3 or PRICKLE4 (green), Alexa 647 phalloidin (647Ph) (red), and Hoechst 33342 (H33342) (blue). (**A**) Proliferation zone. Merged image of staining for PRICKLE3, H33342, and 647Ph. Basement membrane of outer enamel epithelium (OEE) is brightly fluorescent, although its significance is unclear. (**B, E**) Inner enamel secretory ameloblasts. Merged images of staining for PRICKLE3 and H33342 (**B**), and for PRICKLE4, 647Ph, and H33342 (**E**). Anti-PRICKLE3 is positive at the outer enamel epithelia (OEE), stellate reticulum (SR) and stratum intermedium (SI). In secretory ameloblasts (AM in **B**), thread-like fluorescence is visible along the long cell axis. Anti-PRICKLE4 labeled inner enamel-secretory ameloblasts (AM) except for Tomes' processes (TP) as a straight thread-like pattern (**E**). Odontoblasts (OD) are labeled strongly with anti-PRICKLE4 (**E**). (**C, F, G**) Early maturation ameloblasts and papillary layer cells (PL) (**C, G**) and transitional ameloblasts (**F**). Cytoplasm of maturation ameloblast is weakly labeled with anti-PRICKLE3 and anti-PRICKLE4 (**C, G**). Transitional ameloblasts (TA) and osteoblasts (OB) of alveolar bone are strongly labeled with anti-PRICKLE4 (**F**). Singular cells besides the dentin (DE) are strongly labeled with anti-PRICKLE3 (arrow in **D**). PEL: periodontal ligaments. DE: dentin. Bars=50 μm (**A–E, G**); 150 μm (**F**).

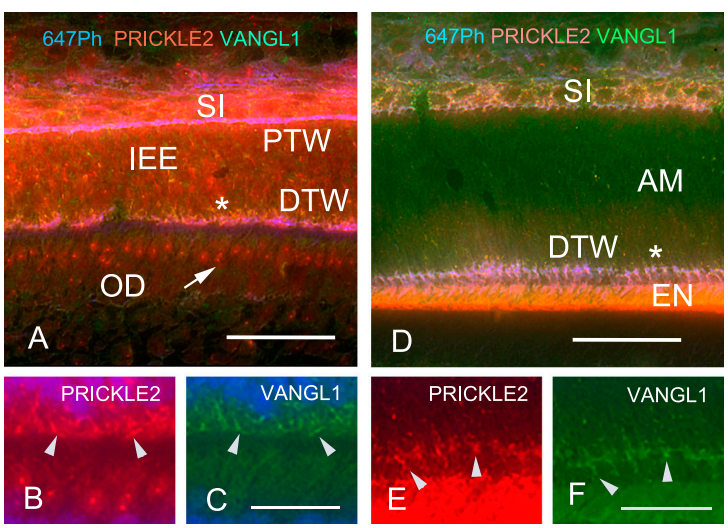

Fig. 3. Triple labeling with anti-VANGL1 (green in **A, C, D**, and **F**), anti-PRICKLE2 (red in **A, B, D**, and **E**), Alexa Fluor 647 phallodin (647Ph) (blue in **A, D**), and Hoechst 33342 (H33342) (blue in **B, C**) of differentiating inner enamel epithelia (IEE) (**A–C**) and inner enamel-secretory ameloblasts (AM) (**D–F**). Nine-day-old rats without fixation and demineralization. Merged images (**A, D**) show that cytoplasmic dots and small rods are both labeled with anti-VANGL1 and anti-PRICKLE2, and most of these are co-localized in inner enamel epithelial cells (asterisks in **A** and **D**). Higher magnification of asterisk in **A** or **D** is shown in **B** and **C**, or **E** and **F**, respectively. Arrowheads in **B** and **C** or **E** and **F** show the same structures. SI, stratum intermedium; OD, odontoblasts; PTW, proximal terminal web; DTW, distal terminal web. Co-localization of these three probes in the DTW results in white color (asterisk in **D**). In odontoblast cytoplasm, anti-PRICKLE2-positive dots are present (arrow in **A**). Bars=50 μm (**A, D**); 20 μm (**C, F**).

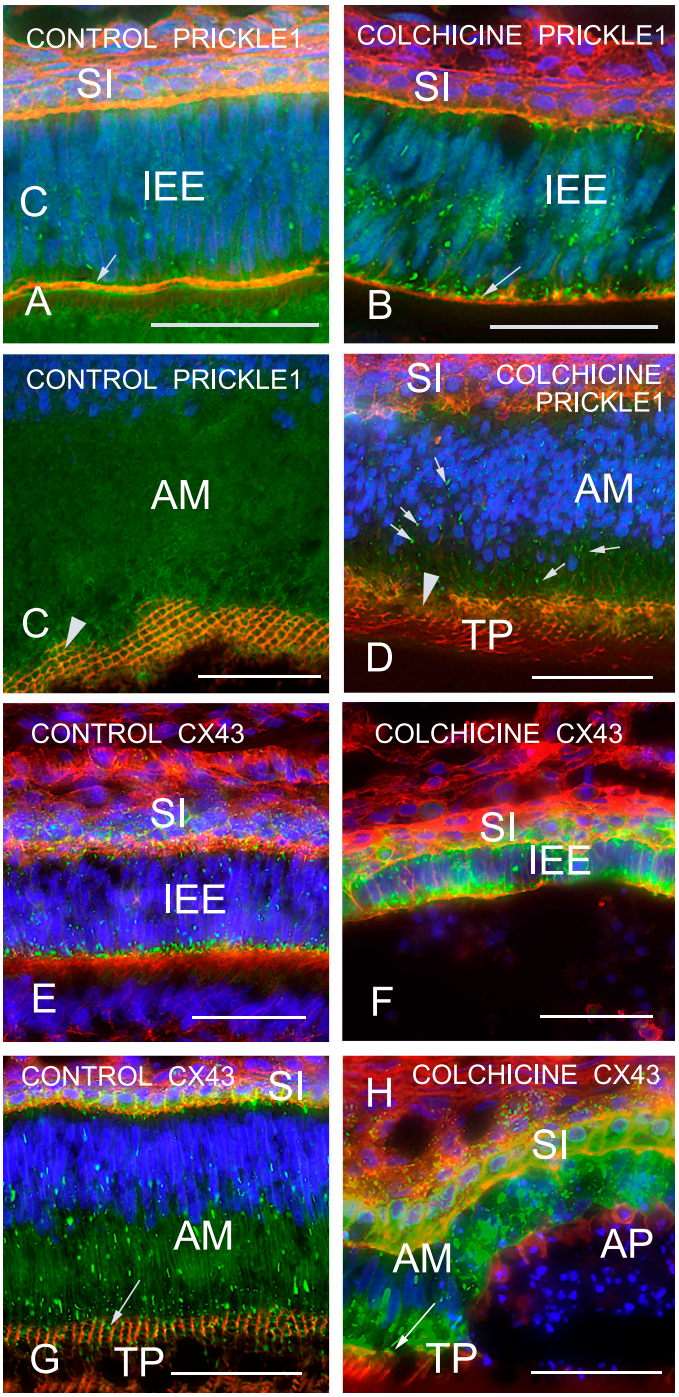

Fig. 4. Triple labeling with anti-PRICKLE1 (green in **A–D**), Alexa 647 phalloidin (red in **A–D**), and Hoechst 33342 (blue in **A–D**), and triple labeling with anti-CX43 (green in **E–H**), Alexa 647 phalloidin (red in **E–H**), and Hoechst 33342 (blue in **E–H**). Four-week-old rats fixed with paraformaldehyde and demineralized with EDTA. Anti-PRICKLE1 and anti-CX43 localization in inner enamel epithelial cells (IEE) of differentiating zone (**A, B, E, F**) and inner enamel-secretory ameloblasts of secretion zone (**C, D, G, H**) in control rats (**A, C, E, G**) and rats treated with colchicine for 15 hr (**B, D, F, H**). Stratum intermedium cells (SI) show some anti-PRICKLE1-positive dots (**A, B, D**) and numerous anti-CX43-positive dots (**E–H**) both in control and colchicine-treated rats. Although some PRICKLE1-derived dots are co-localized with distal junctional complex (arrows in **A, B**), most dots are localized in the supranuclear region both in control and colchicine-treated cells. Inner enamel-secretory ameloblasts treated with colchicine for 15 hr show anti-PRICKLE1-positive dots in supranuclear region (arrows in **D**), and sometimes lack the distal junctional complex (arrowheads in **D**), whereas small PRICKLE1-immunopositive dots are rare in the supranuclear region of ameloblasts (AM in **C**) of the control rat. Distal junctional complexes of inner enamel secretory ameloblasts are positive for anti-PRICKLE1 in the control rat (arrowheads in **C**). Small or medium-sized dots or rods are positive for anti-CX43 in supranuclear cytoplasm of inner enamel epithelial cells and ameloblasts in both control and colchicine-injected rats (**E–H**). Distal junctional complexes of ameloblasts are labeled with anti-CX43 both in control and colchicine-treated rats (arrows in **G** and **H**). Degenerated apoptotic ameloblasts (AP in **H**) are not labeled with anti-CX43 or Alexa647-phalloidin. Bars=50 μm.

33]. Golgi-derived vesicles containing CX43 are transported to the plasma membrane by microtubules and form gap junctions [12, 13]. To examine membrane-bound protein transportation in ameloblasts, colchicine-treated animals were examined. In control animals, numerous CX43-immunoreactive small dots were detected in stratum intermedium cells facing differentiating pre-ameloblasts and secretory ameloblasts (Fig. 4E, G). Numerous cytoplasmic CX43-immunoreactive dots or elongated bars are characteristic in differentiating pre-ameloblasts (Fig. 4E) and secretory ameloblasts (Fig. 4G). CX43-immunoreactive dots were distributed in PTW and DTW, in addition to cytoplasm in inner enamel- to outer enamel-secretory ameloblasts. These patterns were unchanged at 15 and 39 hr after colchicine injection, although some detachment of the ameloblast layer from the enamel surface and frequent apoptosis of ameloblasts were evident (Fig. 4F, H). Colchicine-treated secretory ameloblasts showed a partially disorganized DTW, where Alexa Fluor 647 fluorescence and CX43 immunofluorescence were decreased (Fig. 4H, arrow).

IV. Discussion

In this study, localization of a group of core planar cell polarity proteins (PRICKLE1, PRICKLE2, PRICKLE3, and PRICKLE4) was examined by immunohistochemistry combined with thin frozen sections of non-fixed and undecalcified specimens. All of the antibodies against PRICKLEs showed localization of PRICKLEs in the ameloblasts, but the distribution patterns were different. The present study clearly demonstrated the involvement of core PCP proteins in amelogenesis.

Ameloblasts differentiate from inner enamel epithelial cells. They secrete enamel matrix proteins and exhibit elaborate specific enamel rod alignment. In rat incisor, the inner layer of enamel consists of decussating enamel rod rows and the outer layer of enamel consists of straight-coursed enamel rods. These differing arrangement patterns of enamel rods are due to the medial-lateral movement of ameloblast rows in inner enamel secretion and cessation of this sideways movement in outer enamel secretion, respectively [15, 16, 18, 29]. Along the sliding plane of alternative sideways movement of inner enamel secretory ameloblast rows at the level of the DTW, dense actomyosin filament bundles and adherens junctions are marked, whereas the perpendicular plane within a row exhibits poor actomyosin filaments and adherens junctions [17]. To produce this anisotropic distribution of actomyosin in inner enamel secretory ameloblasts, core PCP proteins are highly likely to play a role, because downstream effectors of FZD and DVL cause actin cytoskeleton reorganization. Our previous work demonstrated the localization of VANGL1, VANGL2, and FZD3 in ameloblasts [21]. From genome-wide transcript profiling of rat incisor, down-regulation of PRICKLE1 gene expression in the maturation zone when compared with the secretion zone has been reported [11], and this is consistent with the results of the present study.

In this study, all PRICKLE proteins were detected by immunohistochemistry. The relationship between PRICKLE3 and planar cell polarization of ameloblasts is unclear, as PRICKLE3 was localized in supranuclear cytoplasm and central cytoplasm at the distal terminal web, but not in the terminal web itself. Contribution of cells other than ameloblasts to enamel organ epithelial cell polarization is, however, possible. PRICKLE3 is reported to be localized in centrioles [6], and the localization pattern in this study was different. PRICKLE4 was localized in the supranuclear cytoplasm of secretory and early maturation ameloblasts, but neither in the proximal and distal terminal web nor in Tomes' processes. Thus, it is unlikely that PRICKLE4 plays a role in planar polarization of ameloblasts. It is interesting to note that PRICKLE4 was localized in hard tissue-forming cells such as odontoblasts and osteoblasts, in addition to ameloblasts. This implies that PRICKLE4 is involved in mineralization-related functions.

PRICKLE1 and PRICKLE2 showed similar localization in the differentiating inner enamel epithelial cells and early inner enamel-secretory ameloblasts, although in later secretion and maturation zones, PRICKLE1 decreased. However, PRICKLE2 showed strong immunoreactivity up to the maturation zone, implying some fine control mechanisms for PRICKLE proteins, as suggested in Drosophila [2, 22]. Pathological effects of planar polarity protein mutation have also been suggested, as some epilepsy patients have been shown to have heterozygous mutations in PRICKLE1 or PRICKLE2 [30].

CX43 is extensively localized in the enamel organ. Numerous dots can be seen in the cytoplasm of stratum intermedium cells, and a punctate pattern is seen in the supranuclear region of differentiating inner enamel epithelial cells, with a tendency to target to distal junctions [3, 5, 8, 32]. As this pattern is similar to PRICKLE1, PRICKLE2, and VANGL1, and as CX43 is known to be transported from the Golgi complex to the plasma membrane by microtubules [4, 13, 27], CX43, PRICKLE1, and PRICKLE4 localization was compared after treatment with the antimitotic drug, colchicine. However, the results showed numerous CX43-derived dots or ovals in both colchicine-treated and control animals. This may be due to the slow turnover rate of distal and proximal junctions where gap junctions are present. In this case, stable gap junctions of ameloblasts are maintained. Conversely, ameloblast gap junctions may exhibit rapid turnover, and the CX43 localization after colchicine treatment in this study may indicate the recovery phase. Gap junction protein turnover rate has been reported to be a few hours [12]. Alternatively, most of the large CX43-positive dots and ovals may indicate connexosomes or annular gap junctions, which are internalized from the intercellular junctional area for degradation processes [12]. Although PRICKLE4 was localized in the cytoplasm of ameloblasts both in colchicine-treated and in

control animals, PRICKLE1 showed different patterns in secretory ameloblasts between colchicine-treated and control animals. PRICKLE1 exhibited increased cytoplasmic labeling as fluorescent dots and decreased fluorescence at the terminal web region, whereas control rat ameloblasts exhibited terminal web immunoreactivity for PRICKLE1 and decreased cytoplasmic labeling. These results suggest the suppression of the transport of hypothetical PRICKLE1-attached vesicles towards the terminal web and cell junctions by microtubules. Disruption of part of the distal terminal web arrangement indicates the involvement of PRICKLE1 in the maintenance of the web pattern.

On the transport of planar cell polarity proteins, Frizzled-containing vesicles have been transported to target plasma membrane via microtubules in Drosophila [28]. In addition, Prickle and Prickle isoform, spiny-legs, in Drosophila have been reported to control microtubule polarity, which is essential for vesicle transport [2, 22].

After colchicine treatment, secretory ameloblasts often detach from the enamel surface and numerous round apoptotic cells persist between ameloblasts and enamel [19]. These round apoptotic ameloblasts were found to lose CX43 reactivity in addition to their columnar shape. In contrast, ameloblasts detached from enamel exhibited CX43 reactivity, thus suggesting stable gap junction persistence in ameloblasts.

In conclusion, PRICKLE2, and probably PRICKLE1, bind to VANGL1, which may target transport to proximal and distal junctions via membrane vesicles in ameloblasts, and may contribute to the polarized anisotropic distribution of distal terminal web and junctions with other core planar cell polarity proteins in inner enamel secretory ameloblasts, and furthermore, may play a role in rat enamel rod architecture. PRICKLE3 and PRICKLE4 showed cytoplasmic labeling in ameloblasts and other enamel organ epithelial cells, although their functional role remains to be clarified.

V. Declaration of Conflicting Interests

The authors declare there are no potential conflicts of interest that may be related to the content of the manuscript, including funding, employment, or personal financial interests.

VI. References

1. Bartlett, J. D., Dobeck, J. M., Tye, C. E., Perez-Moreno, M., Stokes, N., Reynolds, A. B., Fuchs, E. and Skobe, Z. (2010) Targeted p120-catenin ablation disrupts dental enamel development. *PLoS ONE* 5; e12703. doi:10.1371/journal.pone.0012703.
2. Ehaideb, S. N., Iyengar, A., Ueda, A., Iacobucci, G. J., Cranston, C., Bassuk, A. G., Gubb, D., Axelrod, J. D., Gunawardena, S., Wu, C.-F. and Manak, J. R. (2014) *prickle* modulates microtubule polarity and axonal transport to ameliorate seizures in flies. *Proc. Natl. Acad. Sci. U S A* 111; 11187–11192.
3. Fried, K., Mitsiadis, T. A., Guerrier, A., Haegerstrand, A. and Meister, B. (1996) Combinatorial expression patterns of the connexins 26, 32, and 43 during development, homeostasis, and regeneration of rat teeth. *Int. J. Dev. Biol.* 4; 985–995.
4. Harris, T. J. C. and Tepass, U. (2010) Adherens junctions: from molecules to morphogenesis. *Nat. Rev. Mol. Cell Biol.* 11; 502–514.
5. Inai, T., Nakamura, K., Kurisu, K. and Shibata, Y. (1997) Immunohistochemical localization of connexin43 in the enamel organ of the rat upper incisor during ameloblast enamel organ of the rat upper incisor during ameloblast development. *Arch. Histol. Cytol.* 60; 297–306.
6. Jakobsen, L., Vanselow, K., Skogs, M., Toyoda, Y., Lundberg, E., Poser, I., Falkenby, L. G., Bennetzen, M., Westendorf, J., Nigg, E. A., Uhlen, M., Hyman, A. A. and Andersen, J. S. (2011) Novel asymmetrically localizing components of human centrosomes identified by complementary proteomics methods. *EMBO J.* 30; 1520–1535.
7. Jenny, A., Darken, R. S., Wilson, P. A. and Mlodzik, M. (2003) Prickle and Strabismus form a functional complex to generate a correct axis during planar cell polarity signaling. *EMBO J.* 22; 4409–4420.
8. Josephsen, K., Takano, Y., Frische, S., Praetorius, J., Nielsen, S., Aoba, T. and Fejerskov, O. (2010) Ion transporters in secretory and cyclically modulating ameloblasts: a new hypothesis for cellular control of preeruptive enamel maturation. *Am. J. Physiol. Cell Physiol.* 299; C1299–C1307.
9. Kallenbach, E. (1973) The fine structure of Tomes' process of rat incisor ameloblasts and its relationship to the elaboration of enamel. *Tissue Cell* 5; 501–524.
10. Kawamoto, T. (2003) Use of a new adhesive film for the preparation of multi-purpose fresh-frozen sections from hard tissues, whole-animals, insects and plants. *Arch. Histol. Cytol.* 66; 123–143.
11. Lacruz, R. S., Smith, C. E., Bringas, Jr. P., Chen, Y.-B., Smith, S. M., Snead, M. L., Kurtz, I., Hacia, J. G., Hubbard, M. J. and Paine, M. L. (2012) Identification of novel candidate genes involved in mineralization of dental enamel by genome-wide transcript profiling. *J. Cell Physiol.* 27; 2264–2275.
12. Laird, D. W. (2009) The gap junction proteome and its relationship to disease. *Trends Cell Biol.* 20; 92–101.
13. Lauf, U., Giepmans, B. N. G., Lopez, P., Braconnot, S., Chen, S.-C. and Falk, M. M. (2002) Dynamic trafficking and delivery of connexons to the plasma membrane and accretion to gap junctions in living cells. *Proc. Natl. Acad. Sci. U S A* 99; 10446–10451.
14. Lin, M., Li, L., Liu, C., Liu, H., He, F., Yan, F., Zhang, Y. and Chen, Y.-P. (2011) Wnt5a regulates growth, patterning, and odontoblast differentiation of developing mouse tooth. *Dev. Dyn.* 240; 432–440.
15. Nishikawa, S. and Kitamura, H. (1986) Localization of actin during differentiation of the ameloblast, its related epithelial cells and odontoblasts in the rat incisor using NBD-phallacidin. *Differentiation* 30; 237–243.
16. Nishikawa, S., Fujiwara, K. and Kitamura, H. (1988) Formation of the tooth enamel rod pattern and the cytoskeletal organization in secretory ameloblasts of the rat incisor. *Eur. J. Cell Biol.* 47; 222–232.
17. Nishikawa, S., Tsukita, S., Tsukita, S. and Sasa, S. (1990) Localization of adherens junction proteins along the possible sliding interface between secretory ameloblasts of the rat incisor. *Cell Struct. Funct.* 15; 245–249.
18. Nishikawa, S. (1992) Correlation of the arrangement pattern of enamel rods and secretory ameloblasts in pig and monkey teeth: a possible role of the terminal webs in ameloblast movement during secretion. *Anat. Rec.* 232; 466–478.
19. Nishikawa, S. (2002) Colchicine-induced apoptosis and anti-Fas localization in rat incisor ameloblasts. *Anat. Sci. Int.* 77; 175–181.

20. Nishikawa, S. (2004) Cystatin C-positive macrophages and dendritic cells in the rat incisor pulp. *Acta Histochem. Cytochem.* 37; 313–318.
21. Nishikawa, S. and Kawamoto, T. (2012) Planar cell polarity protein localization in the secretory ameloblasts of rat incisors. *J. Histochem. Cytochem.* 60; 376–385.
22. Olofsson, J., Sharp, K. A., Matis, M., Cho, B. and Axelrod, J. D. (2014) Prickle/spiny-legs isoforms control the polarity of the apical microtubule network in planar cell polarity. *Development* 141; 2866–2874.
23. Peng, L., Dong, G., Xu, P., Len, L. B., Wang, C. L., Aragon, M., Zhou, X. D. and Ye, L. (2010) Expression of Wnt5a in tooth germs and the related signal transduction analysis. *Archs. Oral Biol.* 55; 108–114.
24. Sasaki, T., Higashi, S., Tachikawa, T. and Yoshiki, S. (1981) Morphogenesis of gap junctions in rat amelogenesis. *J. Electron Microsc.* 30; 191–197.
25. Sasaki, T. and Garant, P. R. (1986) Fate of annular gap junctions in the papillary cells of the enamel organ in the rat incisor. *Cell Tissue Res.* 246; 523–530.
26. Seifert, J. R. K. and Mlodzik, M. (2007) Frizzled/PCP signalling: a conserved mechanism regulating cell polarity and directed motility. *Nat. Rev. Genet.* 8; 126–138.
27. Shaw, R. M., Fay, A. J., Puthenveedu, M. A., von Zastrow, M., Jan, Y. N. and Jan, L. Y. (2007) Microtubule plus-end-tracking proteins target gap junctions directly from the cell interior to adherens junctions. *Cell* 128; 547–560.
28. Shimada, Y., Yonemura, S., Ohkura, H., Strutt, D. and Uemura, T. (2006) Polarized transport of Frizzled along the planar microtubule arrays in Drosophila wing epithelium. *Dev. Cell* 10; 209–222.
29. Smith, C. E. and Nanci, A. (1996) Protein dynamics of amelogenesis. *Anat. Rec.* 245; 186–207.
30. Tao, H., Manak, J. R., Sowers, L., Mei, X., Kiyonari, H., Abe, T., Dahdaleh, N. S., Yang, T., Wu, S., Chen, S., Fox, M. H., Gurnett, C., Montine, T., Bird, T., Shaffer, L. G., Rosenfeld, J. A., McConnell, J., Madan-Khetarpal, S., Berry-Kravis, E., Griesbach, H., Saneto, R. P., Scott, M. P., Antic, D., Reed, J., Boland, R., Ehaideb, S. N., El-Shanti, H., Mahajan, V. B., Ferguson, P. J., Axelrod, J. D., Lehesjoki, A.-E., Fritzsch, B., Slusarski, D. C., Wemmie, J., Ueno, N. and Bassuk, A. G. (2011) Mutations in prickle orthologs cause seizures in flies, mice, and humans. *Am. J. Hum. Genet.* 88; 138–149.
31. Tissir, F. and Goffinet, A. M. (2013) Shaping the nervous system: role of the core planar cell polarity genes. *Nat. Rev. Neurosci.* 14; 525–535.
32. Toth, K., Shao, Q., Lorentz, R. and Laird, D. W. (2010) Decreased levels of Cx43 gap junctions result in ameloblast dysregulation and enamel hypoplasia in Gja1Jrt/+ mice. *J. Cell Physiol.* 223; 601–609.
33. Walck-Shannon, E. and Hardin, J. (2014) Cell intercalation from top to bottom. *Nat. Rev. Mol. Cell Biol.* 15; 34–48.
34. Wang, B., Li, H., Liu, Y., Lin, X., Lin, Y, Wang, Y., Hu, X. and Zhang, Y. (2014) Expression patterns of WNT/β-CATENIN signaling molecules during human tooth development. *J. Mol. Hist.* 45; 487–496.
35. Warshawsky, H. and Smith, C. E. (1974) Morphological classification of rat incisor ameloblasts. *Anat. Rec.* 179; 423–446.
36. Yuan, X. and Nishikawa, S. (2014) Angular distribution of cross-sectioned cell boundaries at the distal terminal web in differentiating preameloblasts, inner enamel secretory ameloblasts and outer enamel secretory ameloblasts. *Microscopy* 63; 33–39.